Nikolai P. Osipovich, Sergei K. Poznyak, Vladimir Lesnyak, Nikolai Gaponik

**Cyclic voltammetry as a sensitive method for in situ probing of chemical transformations in quantum dots**

Diese Version ist verfügbar / This version is available on:

https://nbn-resolving.org/urn:nbn:de:bsz:14-qucosa2-364191

SLUB
Wir führen Wissen.

TECHNISCHE
UNIVERSITÄT
DRESDEN

QUCOSA
Quality Content of Saxony

CrossMark
click for updates

# Cyclic voltammetry as a sensitive method for *in situ* probing of chemical transformations in quantum dots†

Nikolai P. Osipovich,[a] Sergei K. Poznyak,[a] Vladimir Lesnyak*[b] and Nikolai Gaponik*[b]

The application of electrochemical methods for the characterization of colloidal quantum dots (QDs) attracts considerable attention as these methods may allow for monitoring of some crucial parameters, such as energetic levels of conduction and valence bands as well as surface traps and ligands under real conditions of colloidal solution. In the present work we extend the applications of cyclic voltammetry (CV) to *in situ* monitoring of degradation processes of water-soluble CdTe QDs. This degradation occurs under lowering of pH to the values around 5, *i.e.* under conditions relevant to bioimaging applications of these QDs, and is accompanied by pronounced changes of their photoluminescence. Observed correlations between characteristic features of CV diagrams and the fluorescence spectra allowed us to propose mechanisms responsible for evolution of the photoluminescence properties as well as degradation pathway of CdTe QDs at low pH.

## Introduction

Photoluminescence (PL) is one of the most attractive and practically applicable features of semiconductor nanocrystals (or quantum dots (QDs)). Therefore, many investigations of the PL dependence on various factors have been carried out during the past few decades. Thus, by using PL spectroscopy the influence of various biochemical buffers as well as different metal ions on thiol-stabilized CdTe nanocrystals was recently examined.[1,2] In these experiments one would like to study the PL stability and corresponding chemical stability of QDs in different media (in particular, aerobic and anaerobic ones), and the effect of the medium pH on their optical properties. It is strongly related to the possibility of application of QDs in oxygen saturated aqueous environments.

For CdTe QDs stabilized with thioglycolic (TGA) and mercapto-propionic (MPA) acids it was shown that as the pH decreases their PL increases till a threshold pH is reached, after which PL drops with subsequent aggregation and precipitation of the particles

from solution.[2–6] The PL increase is attributed to the passivating properties of the TGA shell being improved upon pH decreasing owing to a formation and deposition of Cd–thiol complexes on the surface of nanocrystals.[3] Leubner *et al.* demonstrated that a small amount of these Cd–thiolates results in a compact ligand shell, which renders QDs sensitive to fluorescence quenching upon dilution due to ligand adsorption–desorption equilibria. Increasing the ratio of Cd–thiolates to Te suppresses this quenching effect due to the formation of a large shell of complex Cd–thiolate networks around the inorganic core.[7] As shown by Gao *et al.*, when removing the unreacted Cd-precursor and TGA from a QD solution, the PL increase is less pronounced as the pH decreases, with no PL enhancement observed in the thoroughly purified colloid.[3] Furthermore, the acid–base properties of the stabilizer affect the particular trend of the PL dependence on the pH of the media. There are different trends for TGA- and MPA-stabilized CdTe QDs, and when thioglycerol, mercaptoethanol and mercaptoethylamine were used as stabilizers, PL monotonically decreased upon decreasing pH.[3,6]

In this work we provide an insight into the processes occurring at the CdTe QD-solution interface under critical conditions of degradation, combining results of *in situ* PL and cyclic voltammetry (CV) measurements. The latter technique has been widely employed during the last decade to study the electrochemical properties of different kinds of QDs, though mostly CdSe and CdTe ones.[8–15] Lately, we have demonstrated the applicability of the CV for probing energy levels in Hg-doped CdTe QDs supported by density functional theory calculations.[16] This method is especially sensitive to surface related processes, in particular, to reactions of ligand molecules. To elucidate these

[a] *Research Institute for Physical Chemical Problems, Belarusian State University, Leningradskaya Str. 14, 220030 Minsk, Belarus*

[b] *Physical Chemistry, TU Dresden, Bergstr. 66b, 01062 Dresden, Germany. E-mail: vladimir.lesnyak@chemie.tu-dresden.de, nikolai.gaponik@chemie.tu-dresden.de*

† Electronic supplementary information (ESI) available: Additional voltammo-grams of Au electrodes with adsorbed CdTe QDs, and voltammograms of thin film Te, Te-terminated and Cd-terminated CdTe electrodes. See DOI: 10.1039/c6cp01085g

This journal is © the Owner Societies 2016

*Phys. Chem. Chem. Phys.,* 2016, **18**, 10355–10361 | **10355**

processes we compared electrochemical behaviour of the QDs with that of bulk CdTe and Te films under similar conditions.

## Experimental section

TGA-stabilized CdTe QDs were synthesized according to the reported procedure.[17–19] CdTe QD colloids with average particle sizes of 2.0, 2.8 and 3.5 nm were selected for the investigation. Temporal evolution of the PL properties of CdTe QDs was studied in an acetate buffer solution with pH 5 (0.1 M $CH_3COONa$ + 0.0468 M $CH_3COOH$) in contact with air and after deaeration by purging argon for 1 h.

Electrochemical measurements were performed in a standard three-electrode two-compartment cell with a platinum counter-electrode and a Ag|AgCl|KCl(sat.) electrode as the reference electrode (+0.201 V $vs.$ SHE). All potentials were determined with respect to this reference electrode and were controlled using an Autolab PGSTAT 302N potentiostat. Potentiodynamic polarization was performed at a potential sweep rate of 20 mV s$^{-1}$. The working electrode compartment of the electrochemical cell was separated from the counter-electrode compartment by a fine porous glass membrane. Gold plates were used as working electrodes. The surface of the gold plates was polished by diamond paste followed by treatment in boiling concentrated $HNO_3$ and $H_2SO_4$. Then the gold electrodes were thoroughly washed with doubly distilled water and annealed at 700 °C for 20 min in air. The cleaned electrodes were dipped into the deaerated colloidal solutions of CdTe QDs for 5 min, which resulted in their adsorption on the electrode surface.[20] The electrodes with adsorbed QDs (CdTe QDs|Au) were then washed with doubly distilled water and transferred to the electrochemical cell. The current and charge values are given for the geometric electrode surface area. Detailed characterisation of the CdTe QDs|Au electrodes, including estimation of the particle loading per surface area, can be found in ref. 20.

Electrochemical measurements were carried out in an acetate buffer solution (pH 5) after its deaeration by purging argon for 30 min. Analytical-grade reagents and doubly distilled water were used for the electrolyte preparation.

CdTe thin film electrodes used for the examination of electrochemical behaviour of cadmium telluride were deposited at −0.3 V ($vs.$ Ag|AgCl|KCl$_{sat.}$) on a gold foil from 1 mM $TeO_2$ + 1 M $CdSO_4$ + 0.05 M $H_2SO_4$ solution at 70 °C, similar to the previously reported procedure for CdTe electrodeposition (see Fig. S1 in the ESI† for a photo of the film and its scanning electron microscopy image).[21–23] The estimated thickness of the deposited CdTe layer was about 30 nm, assuming 100% coulomb efficiency of the process. Te-terminated and Cd-terminated surfaces of CdTe thin film electrodes were produced by the following methods based on the results of the investigations of CdTe electrochemistry.[24] To prepare Te-terminated CdTe, the electrode was kept for 2 min in the electrolyte after electrodeposition, where tellurium atoms on the CdTe surface substituted cadmium atoms as a result of exchange processes. To produce Cd-terminated CdTe, the CdTe thin film electrode was removed

from the cell after deposition, rinsed with water and dipped into another electrochemical cell with the 0.01 M $Cd(ClO_4)_2$ + $HClO_4$ electrolyte (pH 1) where it was polarized at −0.45 V for 8 min. Under these conditions underpotential deposition of cadmium ad-atoms occurred on surface tellurium atoms, resulting in a Cd-terminated surface. Formation of the Cd-terminated and Te-terminated CdTe surfaces was previously supported by both electrochemical methods and elemental analysis of the products of electrochemical dissolution of an upper monolayer from the CdTe surface.[23] Te films, used to study the electrochemical behaviour of Te, were deposited on a gold substrate from 1 mM $TeO_2$ + 0.05 M $H_2SO_4$ solution.

As TGA was used to stabilize CdTe QDs, electrochemical behaviour of TGA adsorbed on the surface of Au and CdTe thin film electrodes was also examined. To adsorb TGA, the electrodes were dipped into 0.002 M TGA solution for 2 min, then rinsed with water and placed into the electrochemical cell.

## Results and discussion

### Electrochemical behaviour of CdTe QDs adsorbed on the Au electrode in acetate buffer

Prior to electrochemical measurements we tested the stability of CdTe QDs in acetate buffer with pH 5. Absorption and PL spectra of QD colloids of three different sizes are presented in Fig. 1a and b. 2.8 nm QDs were chosen as a representative sample for testing. As shown in Fig. 1c, the PL intensity of this CdTe QD colloid was found to decay immediately after addition into an aerated acetate buffer, becoming undetectable within several minutes. In contrast, in deaerated buffer solution the PL intensity was much more stable, and even demonstrated the tendency for enhancing during first hour after mixing.
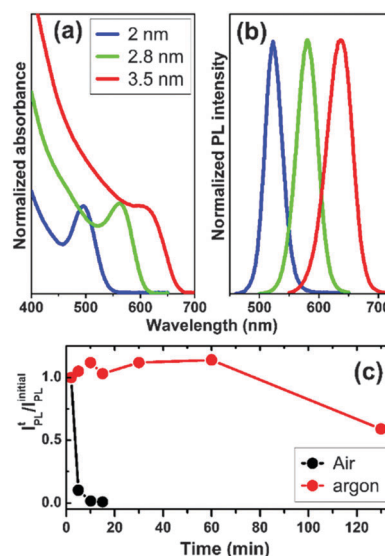


**Fig. 1** Absorption (a) and PL (b, $\lambda_{ex}$ = 450 nm) spectra of aqueous solutions of CdTe QDs with sizes of 2.0, 2.8 and 3.5 nm. (c) Temporal evolution of the relative PL intensity $I_{PL}^t/I_{PL}^{initial}$ of 2.8 nm CdTe QD colloids in an acetate buffer (pH 5) under air and deaerated by argon bubbling ($\lambda_{ex}$ = 450 nm).

Only after one hour the PL intensity began to drop, which can be associated with QD coagulation and precipitation.

Furthermore, in electrochemical experiments we acquired cyclic voltammograms of a bare Au electrode and Au electrode with adsorbed TGA in acetate buffer as control samples to extract their background responses (see Fig. 2a). Oxidation of the Au electrode surface (the anodic wave $A^{Au}$) upon anodic polarization begins from 0.85 V, whereas the cathodic peak $C^{Au}$ corresponds to its reduction upon the reverse scan. In the case of the Au electrode with adsorbed TGA the latter begins to oxidize from 0.35 V, reaching the current peak at 0.97 V ($A^{TGA}$) and then dropping. After TGA oxidation upon the next scan the voltammogram is similar to that of the pure Au electrode (Fig. 2a, second scan, green line).

The anodic voltammogram of the CdTe QD|Au-electrode immersed into acetate buffer exhibits two peaks of QD oxidation, $A_1$ and $A_2$ (Fig. 2b, black line). Previously we also observed two anodic peaks upon oxidation of CdTe QDs adsorbed on the Au surface in alkaline buffer solution at pH 9.2, and attributed them to oxidation of the surface trap states and of the core.[20] As compared to pH 9.2, at pH 5 the peak $A_2$ is shifted in the positive direction because the electrochemical process depends on pH. It should be noted that by keeping the CdTe QD|Au-electrode in acetate buffer (pH 5) under open circuit conditions, its potential (open circuit potential, $E_{OC}$) drifts in the negative direction (from initial $-0.14$ V to $-0.24$ V in 15 min), whereas at pH 9.2 this drift was almost negligible. Afterwards, this trend reverses, i.e. $E_{OC}$ begins to shift in the positive direction, reaching $-0.085$ V after 60 min (see Fig. 2b, inset).

Voltammograms of CdTe QD|Au-electrodes recorded after different times of immersion reveal significant changes in the system. Thus, the first anodic peak $A_1$ gradually splits into four peaks $A_1^1$–$A_1^4$ (Fig. 2b). Its charge (the $A_1$ peak charge – the sum of charges of $A_1^1$–$A_1^4$ peaks) first increased (from initial 1.19 mC cm$^{-2}$ up to 1.59 mC cm$^{-2}$ in 5 min), then remained practically constant till 15 min (1.51 mC cm$^{-2}$), and then decreased after 30 min. By 60 min we observed only traces of the most negative $A_1^1$ peak in the voltammogram (Fig. 2b, cyan line).

The potential of the second anodic peak $A_2$ was practically unchanged up to 15 min of immersion, but its charge (the charge of Au surface oxidation belonging to the $A^{Au}$ wave is subtracted) decreased from initial 1.39 mC cm$^{-2}$ down to 1.18 mC cm$^{-2}$ at 5 min, remaining constant for 15 min and then decreasing. We note that initially the peak $A_2$ was sufficiently intensive and masked the $A^{Au}$ wave, rendering it practically invisible. However, after keeping the CdTe QD|Au-electrode in acetate buffer under open circuit conditions for 30 or 60 min, the peaks $A_2$ and $A^{Au}$ began to separate in the voltammograms owing to a drop in the $A_2$ peak intensity (Fig. 2b, blue and cyan lines). The net anodic charge of QD oxidation remained practically unaltered within first 15 min and then decreased. Here we point out that the similar behaviour we observed in the case of 2 nm and 3.5 nm sized CdTe QDs in acetate buffer (see Fig. S2, ESI†).

## Electrochemistry of CdTe thin films terminated with Te and Cd atoms in acetate buffer

As a next step, to get an insight into the nature of the electrochemical behaviour of CdTe QDs, we studied CdTe thin films deposited on gold electrodes as a model system, and in particular the difference in CV responses between Cd- and Te-terminated films.

The surface of CdTe thin films may have three possible states: (i) Te-terminated, (ii) Cd-terminated, and (iii) terminated with Te and Cd atoms in different ratios. Among these cases, Te-terminated and Cd-terminated CdTe were chosen for investigation. Their anodic voltammograms are shown in Fig. S3 (ESI†). Moreover, as TGA is used as a ligand to stabilize CdTe QDs, we also examined the influence of TGA adsorption on the electrochemical behaviour of Te-terminated and Cd-terminated CdTe films. As seen from the CV traces, there is only one peak of Te-terminated CdTe oxidation. The oxidation process begins from +0.2 V reaching the anodic current maximum at +0.5 V. Voltammograms of bare Te-terminated CdTe thin film (solid line) electrodes and those treated by TGA (dashed line) are quite similar within the measurement variation (Fig. S3a, ESI†), suggesting that TGA is not adsorbed on the Te-terminated surface, otherwise its oxidation would have given an additional anodic charge. At the same time, Cd-terminated CdTe thin film electrodes exhibit two peaks of oxidation: one at +0.5 V and an additional anodic peak $A_{CdTe}^{Cd}$ at +0.09 V (see Fig. S3b, ESI†). As was shown,[24] its appearance is related to dissolution of the surface layer of cadmium atoms from CdTe as a result of the electrochemical reaction:

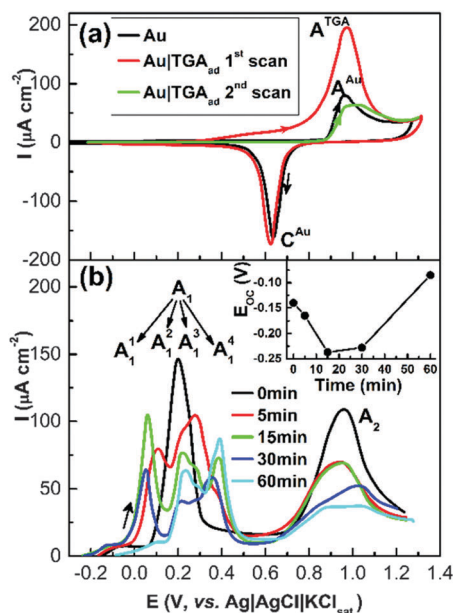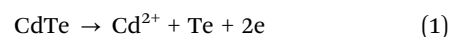$$CdTe \rightarrow Cd^{2+} + Te + 2e \qquad (1)$$



Fig. 2 (a) Voltammograms of the Au electrode and the Au electrode with adsorbed TGA. (b) Anodic voltammograms of Au electrodes with adsorbed 2.8 nm CdTe QDs kept before polarization in an acetate buffer (pH 5) under open circuit conditions for 0, 5, 15, 30 and 60 min. The inset shows the dependence of the open circuit potential, $E_{OC}$, on time. Electrolyte: acetate buffer solution with pH 5.

The voltammogram of the Cd-terminated CdTe thin film electrode treated with TGA demonstrates higher current peaks as compared to those of the non-treated one, implying that TGA is adsorbed on the Cd-terminated CdTe surface, as opposed to the Te-terminated surface. In this case oxidation of adsorbed TGA gives an additional charge.

### Electrochemical behavior of Te thin films

In order to record electrochemical response of Te we deposited its film on the surface of the Au electrode from 1 mM $TeO_2$ + 0.05 M $H_2SO_4$ solution with pH 1 upon the cathodic potential scan from the open circuit potential, since at higher pH values $TeO_2$ has a low solubility. Voltammograms of the Au electrode in $TeO_2$ solution with pH 1 are shown in Fig. S4a (ESI†), they are in agreement with previously published data.[25,26] Upon cathodic scan these voltammograms exhibit two peaks of underpotential deposition of the tellurium monolayer (2D), $C_1^{Te2D}$ and $C_2^{Te2D}$. Deposition of bulk tellurium (Te3D) begins at about +0.05 V. In the reverse scan bulk tellurium has been dissolved first (the corresponding anodic peak $A^{Te3D}$), followed by the dissolution of the Te monolayer (2D) (peaks $A_1^{Te2D}$ and $A_2^{Te2D}$).

In acetate buffer an anodic peak of Te 2D oxidation ($A_1^{Te2D}$) is observed at +0.42 V (Fig. S3b, dotted line, ESI†). On the reverse cathodic scan a peak at 0.105 V corresponds to the reduction of tellurium oxidation products on the Au surface (Fig. S3b, dotted line, ESI†), which results in the formation of a Te layer on the Au surface. When the amount of Te deposited on the Au surface increases up to the stage of Te3D layer formation, the anodic voltammogram of this electrode shows a peak of Te oxidation ($A^{Te3D}$) at +0.28 V and two peaks of Te2D oxidation: $A_2^{Te2D}$ at 0.33 V (a shoulder for peak $A^{Te3D}$) and $A_1^{Te2D}$ at +0.43 V (Fig. S4b, solid line, ESI†). All these peaks are negatively shifted and broadened, as compared to those in solution with pH 1 (see Fig. S3a, ESI†), while the peaks $A^{Te3D}$ and $A_2^{Te2D}$ are almost merged into one. This shift is due to the absence of Te species in the solution and the electrochemical process being dependent on pH, as follows from the Nernst equation. Overall, in both solutions with pH 1 and 5 the patterns of oxidation of Te deposited on the Au electrode are similar. By further increasing the Te amount on the Au surface the charge of tellurium oxidation increases upon anodic polarization (Fig. S4c, ESI†). By reverse cathodic scan, in addition to the $C_1^{Te2D}$ peak at +0.105 V, two more peaks of reduction of oxidized Te species are observed, $C^{Te1}$ and $C^{Te2}$, at −0.17 and from −0.4 to −0.5 V, respectively (Fig. S4c, ESI†).

The phenomenon of underpotential deposition, studied previously at pH 1,[24] is also observed in the course of electro-reduction of cadmium ions on the Te electrode. This is indicated by a peak $C_{Te}^{Cd}$ at −0.46 V corresponding to the following process:

$$Cd^{2+} + 2e \xrightarrow{Te} Cd_{ad}|Te \qquad (2)$$

An anodic peak $A_{Te}^{Cd}$ at −0.15 V (see Fig. S5, ESI†) corresponds to Cd dissolution upon the reverse scan. A shoulder $A^{CdTe}$ at 0.04 V can be assigned to the stripping of the surface layer of cadmium atoms from CdTe as a result of reaction (1). CdTe was formed due to a gradual interaction of the deposited cadmium atoms and tellurium.[24]

### Processes involved in electrochemical oxidation of CdTe QDs

The results of examining electrochemical behaviour of Te and CdTe thin films, and underpotential deposition of Cd on Te in acetate buffer allow us to assign the peaks observed in voltammograms of CdTe QD|Au-electrodes to certain electrochemical processes. The potential of the $A_1^1$ peak coincides with that of the $A_{CdTe}^{Cd}$ peak observed in voltammograms for Cd-terminated CdTe thin film electrodes (cf. Fig. 2b and Fig. SI3b, ESI†), suggesting that the $A_1^1$ peak is also related to oxidation of surface cadmium atoms of CdTe QDs as a result of electrochemical reaction (1). The potential of the $A_1^4$ peak of CdTe QD|Au-electrodes is close to that of the peak of Te2D oxidation on the Au surface, $A_1^{Te2D}$ (cf. Fig. 2b and Fig. S4b and c, ESI†), implying that the $A_1^4$ peak has the same origin as the $A_1^{Te2D}$ peak and is related to tellurium oxidation. An additional insight into the origin of $A_1^1$–$A_1^4$ peaks is obtained by examining the products of anodic oxidation of CdTe QDs upon cathodic scan. To do this, the CdTe QD|Au-electrode was polarized first in the positive direction from $E_{OC}$ to certain potential values, then the direction of polarization was reversed, and detection of products of anodic oxidation of QDs was carried out upon cathodic scan. The results obtained are presented in Fig. 3. As seen from Fig. 3a, after 15 min under open circuit conditions followed by anodic polarization of the electrode from $E_{OC}$, the peak $A_1^1$ was recorded, whereupon the scan direction was reversed and a cathodic peak at −0.4 V was observed in the voltammogram (black line).

Further analysis of voltammograms reveals that the peak of reduction of cadmium ions on tellurium $C_{Te}^{Cd}$ (see Fig. S5, ESI†) and that of reduction of tellurium on gold $C^{Te2}$ (see Fig. S4c, ESI†) have close potentials. However, the anodic peak of the detachment of cadmium ad-atoms from the Te surface, $A_{Te}^{Cd}$ (at −0.33 V), with a typical shoulder on the anodic side ($A^{CdTe}$) suggests that the cathodic peak at −0.4 V belongs to underpotential reduction of cadmium ions on tellurium. $Cd^{2+}$ ions appear in the solution as a result of the process related to the $A_1^1$ peak. Consequently, the peak $A_1^1$ is attributed to Cd dissolution from CdTe QDs. Although the value of −0.33 V for the $A_{Te}^{Cd}$ peak observed for the CdTe QD|Au-electrode is distinctly different from that of −0.15 V for the $A_{Te}^{Cd}$ peak observed on the bulk Te (see Fig. S5, ESI†), we have reported that the potential values for the peaks of dissolution of metal ad-atoms depend on the amount of chalcogen.[27–30] Thus, on mono- and sub-monolayers of chalcogens they are shifted in the negative direction, as compared to the bulk chalcogens.

After the peak $A_1^2$ upon the reverse scan an additional cathodic peak appears in the region from +0.1 to −0.2 V (Fig. 3a, red line). It may be identified with that of tellurium species reduction, $C^{Te1}$. After $A_1^3$ peak current rises sharply, and after $A_1^4$ peak on the reverse scan a peak of deposition of Te ad-atoms on gold, $C_1^{Te2D}$, also appears (Fig. 3a, green and blue lines). Since the

**10358** | *Phys. Chem. Chem. Phys.*, 2016, **18**, 10355–10361

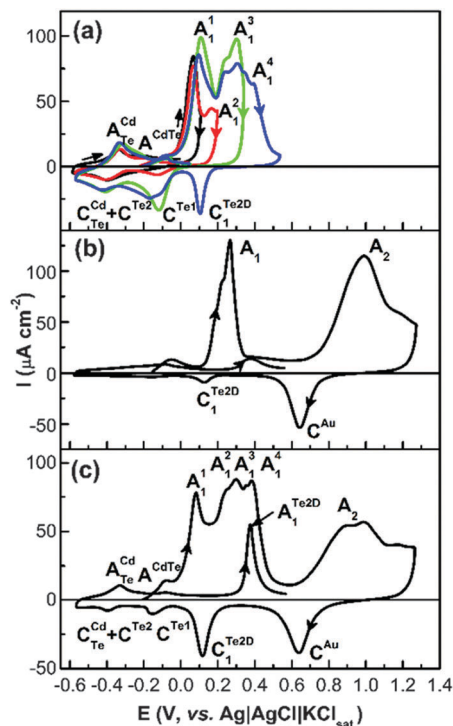This journal is © the Owner Societies 2016

Fig. 3 Voltammograms of 2.8 nm CdTe QD|Au-electrodes kept for 15 min under open circuit conditions before starting polarization (a and c) and immediately immersed into acetate buffer (b). (a) Anodic polarization from $E_{OC}$ to +0.106 V (black line), +0.195 V (red line), +0.339 V (green line), and +0.532 V (blue line), thereafter cathodic polarization to −0.6 V and from −0.6 to 0 V.

peak of Te reduction, $C^{Te2}$, coincides with that of cadmium underpotential deposition, $C_{Te}^{Cd}$, they cannot be observed separately in voltammograms. However, the charge increase in the region of the peak at −0.4 V confirms that the peaks $A_{Te}^{Cd}$ and $C^{Te2}$ are superimposed. Thus, as a result of anodic processes indicated by $A_1^2$, $A_1^3$, and $A_1^4$ peaks, oxidized Te species appear on the electrode surface. Among them the peak $A_1^4$ is related to oxidation of tellurium ad-atoms on the Au electrode surface. Consequently, when the electrode potential approaches a value of the onset potential of the $A_1^4$ peak in the process of polarization, Te3D has already been oxidized leaving just the last monolayer of Te ad-atoms on the Au surface.

As demonstrated experimentally, the electrochemical processes related to the peaks $A_1^2$ and $A_1^3$ involve tellurium oxidation. By this, the ratio of $A_1^1$ peak charge to the total charge of the peaks $A_1^2$, $A_1^3$, and $A_1^4$ is very close to 1 : 2, and is given by two successive electrochemical reactions, reaction (1) and (3):

$$Te + 2H_2O \rightarrow TeO_2 + 4H^+ + 4e \qquad (3)$$
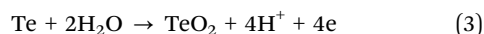
Thus, as a result of electrochemical reaction (1) (the corresponding peak $A_1^1$) the CdTe QD loses Cd and transforms into a Te particle. In this process QDs can be disintegrated into smaller parts (for detailed explanation see the ESI,† Fig. S6 and related comments). Under our experimental conditions practically all cadmium of CdTe QD is involved in reaction (1). After stripping of cadmium, tellurium oxidation goes on, indicated

by the peaks $A_1^2$, $A_1^3$, and $A_1^4$. We note that in the voltammogram of the CdTe QD|Au-electrode recorded immediately after immersion into acetate buffer the peak of Te species reduction, $C_1^{Te2D}$, is small, and the other peaks of Te reduction and the peak of under-potential Cd deposition on tellurium are not registered (Fig. 3b). Upon polarization of the CdTe QD|Au-electrode after 15 min a sharp increase of the peak $C_1^{Te2D}$ is observed, and peaks of tellurium reduction ($C^{Te1}$, $C^{Te2}$) and that of Cd underpotential deposition ($C_{Cd}^{Te}$) appear (see Fig. 3c).

Analysis of these data leads to the following deduction. Since the QDs were brought into contact with the Au surface by the TGA-shell, the probability that upon their anodic oxidation Te species directly interact with the Au surface is quite small (although it is not zero, as evidenced by the presence of the $C_1^{Te2D}$ peak in the voltammogram). In contrast, by keeping the electrode in acetate buffer TGA ligands are eliminated from the QD surface and they directly touch the Au substrate, which leads to a higher probability for tellurium to react with the Au surface upon anodic oxidation. Accordingly, this is reflected in voltammograms as a growth of the $C_1^{Te2D}$ peak, as well as the development of $C^{Te1}$ and $C^{Te2}$ peaks and the peak of Cd underpotential deposition on Te. The possible nature of this transformation will be discussed later.

The peak $A_2$ (this peak also includes the gold oxidation wave as discussed above), as follows from comparison of Fig. 2a and 3, can be related to electrooxidation of TGA. However, the origin of this peak is more complicated, as evidenced by the data presented in Fig. 4. In this experiment two CdTe QD|Au-electrodes were first anodically polarized to +0.52 V, while one of them was kept for 15 min under open circuit conditions before polarization
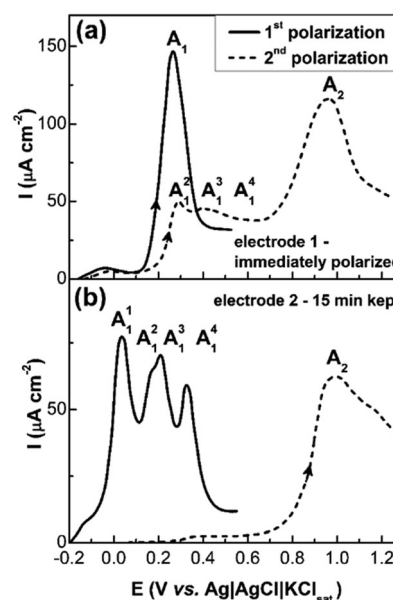


Fig. 4 Anodic voltammograms of the 2.8 nm CdTe QD|Au-electrode, immediately polarized (a) and held for 15 min in acetate buffer under open circuit conditions before polarization (b). Solid lines reflect polarization from the open circuit potential to +0.52 V. Thereafter the electrochemical cell was switched off. After 15 min of immersion under open circuit conditions anodic polarization of the electrodes was switched on again (dashed lines).

This journal is © the Owner Societies 2016

*Phys. Chem. Chem. Phys.*, 2016, **18**, 10355–10361 | **10359**

(electrode 2). In the voltammogram of the immediately polarized electrode (electrode 1) we observed the $A_1$ peak (see Fig. 4a), whereas in the case of electrode 2, peaks $A_1^1$–$A_1^4$ are recorded (Fig. 4b). Afterwards, the cell was switched off, and both electrodes were kept for 15 min in the solution under open circuit conditions. Then the cell was switched on, and the electrodes were again anodically polarized from open circuit potential. In the case of electrode 1, $A_1^2$, $A_1^3$ and $A_1^4$ peaks (belonging to Te oxidation) and the $A_2$ peak were recorded (Fig. 4a), while for the electrode 2 only the $A_2$ peak was observed (Fig. 4b). Therefore, only in the latter case the $A_2$ peak can be identified upon solely TGA oxidation. In the case of immediate polarization both TGA and some part of tellurium were oxidized in the potential range of the $A_2$ peak. This results in a charge redistribution between the peaks $A_1$ (total charge of $A_1^1$–$A_1^4$ components) and $A_2$ as described above (see Fig. 2).

### Mechanism of the pH effect on the electrochemical and luminescence properties of CdTe QDs

The results of the electrochemical studies help us to understand how the solution pH influences the electrochemical and luminescence properties of CdTe QDs. The most consistent explanation of the observed transformations in the electrochemical behavior of CdTe QDs adsorbed on the Au electrode can be proposed by taking into account the results from ref. 31. According to the data of ref. 31, when immersing CdTe QDs into a buffer solution with pH 5, protonation of thiolate sulfur linked to Cd on the particle surface occurs resulting in splitting of Cd–S bonds with subsequent desorption of TGA molecules. After these transformations the particles behave electrochemically as bulk CdTe, establishing the direct contact with the Au electrode surface. However, there are a number of facts which do not fit to the scheme proposed in ref. 31. First, TGA desorption and its diffusion into the solution must result in a decrease of total anodic charge, but for the holding times of up to 15 min no appreciable charge decrease was observed. Second, according to our data, the protonated TGA is not adsorbed on the Te-terminated CdTe surface, but rather on Cd-sites. As a result, even after cleavage of Cd–S bonds TGA should remain adsorbed on the surface of QDs most probably via van der Waals bonding with Cd, as they predominantly have the Cd-terminated CdTe surface.[32] Third, the loss of the ligand would have resulted in PL drop, however in an inert atmosphere PL is maintained for a quite long time.

Therefore, bearing in mind the above discussion we modified the mechanism proposed by Aldana et al. and presented it in Fig. 5. According to this scheme, by immersing the CdTe QD|Au-electrode or pouring an aliquot of QD colloid into the buffer solution with pH 5 protonation and subsequent cleavage of the Cd–S bond occur on the particle surface. Nevertheless, TGA molecules remain on the Cd-terminated surface, although being attached through weaker van der Waals bonds, and thus become more labile. In this way, since the particles in solution retain their ligand shells, their PL is also preserved. However, as a consequence of neutralization of –COO⁻ groups, which are transformed into neutral –COOH groups, zeta potential of the
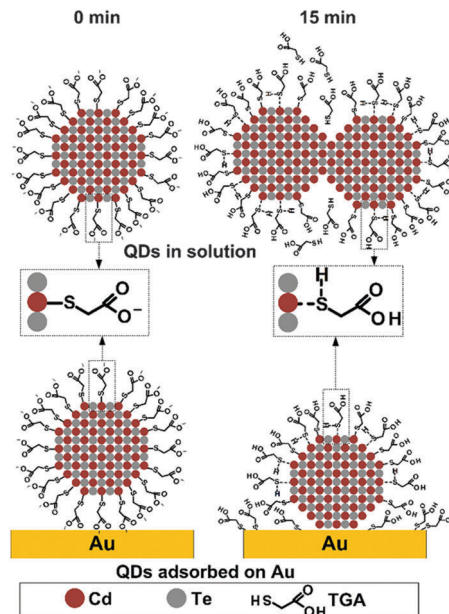


Fig. 5 Scheme of the processes involving CdTe QDs adsorbed on the Au electrode and QDs in acetate buffer solution with pH 5.

QDs decreases, and their electrostatic repulsion becomes smaller leading to their agglomeration.[6] In the case of QDs adsorbed on the surface of the Au electrode, TGA molecules due to their lability also may be driven out of the particles to the surface of gold, which results in a direct contact between QDs and the Au surface. Being weaker, van der Waals bonds have no appreciable stabilizing effect against particle oxidation, as evidenced by the influence of TGA adsorbed on the Cd-terminated CdTe surface. The particles begin to oxidize at much more negative potentials ($A_1^1$ peak location is almost 200 mV more negative than that of the initial $A_1$ peak). This leads to a sharp decrease of CdTe QD stability against oxidation. Due to gradual oxidation the open circuit potential of the CdTe QD|Au-electrode begins to drift in the positive direction after the initial negative shift (Fig. 2b, inset). Traces of oxygen act as an oxidizer in the system with increasing activity as the pH decreases. The equation for the $E$-pH diagram for $O_2/OH^-$ or $O_2/H_2O$ is as follows:[33]

$$E \text{ (V)} = 1.23 - 0.059 \text{ pH} \qquad (4)$$

Upon oxidation the charge of the most negative $A_1^1$ peak decreases with time much faster than those of all the other components of the $A_1$ peak (Fig. 2b). As the peak $A_1^1$ is related to Cd atom stripping, the process leads to enrichment of the particles by Te, resulting in a decrease of the PL quantum yield due to the increase of the number of surface trap states.[32] On the other hand, in an inert atmosphere PL of QDs is retained, but the particles gradually aggregate with time and precipitate eventually resulting in the PL decrease.

## Conclusions

The processes responsible for the pH effect on the chemical stability of TGA capped CdTe QDs and their PL have been

investigated by electrochemical methods under critical conditions. When aqueous CdTe QDs are introduced into a buffer solution with pH 5, thiolic groups are protonated, and Cd–S bonds on the surface are disrupted. This causes the drop of QD stability against oxidation. Nevertheless, TGA molecules remain adsorbed on the Cd-terminated surface of QDs, being anchored to the particle surface by weak van der Waals bonds. Upon oxidation in air, CdTe QDs first lose cadmium, which leads to the excess of tellurium that resulted in a PL quantum yield decrease within several minutes. In contrast, in an inert atmosphere PL of QD solutions is retained, although slowly decreasing with time due to a gradual aggregation of the particles and their precipitation from solution. The results obtained are of interest for different applications of thiol-stabilized QDs, for example, as biomarkers.

## Acknowledgements

## Notes and references

1 K. Boldt, O. T. Bruns, N. Gaponik and A. Eychmüller, *J. Phys. Chem. B*, 2006, **110**, 1959–1963.

2 A. S. Susha, A. M. Javier, W. J. Parak and A. L. Rogach, *Colloids Surf., A*, 2006, **281**, 40–43.

3 M. Gao, S. Kirstein, H. Möhwald, A. L. Rogach, A. Kornowski, A. Eychmüller and H. Weller, *J. Phys. Chem. B*, 1998, **102**, 8360–8363.

4 H. Zhang, Z. Zhou, B. Yang and M. Gao, *J. Phys. Chem. B*, 2003, **107**, 8–13.

5 A. Mandal and N. Tamai, *J. Phys. Chem. C*, 2008, **112**, 8244–8250.

6 S. Xu, C. Wang, H. Zhang, Z. Wang, B. Yang and Y. Cui, *Nanotechnology*, 2011, **22**, 315703.

7 S. Leubner, S. Hatami, N. Esendemir, T. Lorenz, J.-O. Joswig, V. Lesnyak, S. Recknagel, N. Gaponik, U. Resch-Genger and A. Eychmüller, *Dalton Trans.*, 2013, **42**, 12733–12740.

8 M. Amelia, C. Lincheneau, S. Silvi and A. Credi, *Chem. Soc. Rev.*, 2012, **41**, 5728–5743.

9 S. K. Haram, B. M. Quinn and A. J. Bard, *J. Am. Chem. Soc.*, 2001, **123**, 8860–8861.

10 X. Ma, A. Mews and T. Kipp, *J. Phys. Chem. C*, 2013, **117**, 16698–16708.

11 E. Kuçur, W. Bucking, R. Giernoth and T. Nann, *J. Phys. Chem. B*, 2005, **109**, 20355–20360.

12 E. Kuçur, W. Bücking and T. Nann, *Microchim. Acta*, 2008, **160**, 299–308.

13 E. Kuçur, J. Riegler, G. A. Urban and T. Nann, *J. Chem. Phys.*, 2003, **119**, 2333–2337.

14 L. de la Cueva, K. Lauwaet, R. Otero, J. M. Gallego, C. Alonso and B. H. Juarez, *J. Phys. Chem. C*, 2014, **118**, 4998–5004.

15 G. B. Markad, S. Battu, S. Kapoor and S. K. Haram, *J. Phys. Chem. C*, 2013, **117**, 20944–20950.

16 P. P. Ingole, V. Lesnyak, L. Tatikondewar, S. Leubner, N. Gaponik, A. Kshirsagar and A. Eychmüller, *ChemPhysChem*, 2016, **17**, 244–252.

17 N. Gaponik, D. V. Talapin, A. L. Rogach, K. Hoppe, E. V. Shevchenko, A. Kornowski, A. Eychmüller and H. Weller, *J. Phys. Chem. B*, 2002, **106**, 7177–7185.

18 V. Lesnyak, N. Gaponik and A. Eychmüller, *Chem. Soc. Rev.*, 2013, **42**, 2905–2929.

19 A. L. Rogach, T. Franzl, T. A. Klar, J. Feldmann, N. Gaponik, V. Lesnyak, A. Shavel, A. Eychmüller, Y. P. Rakovich and J. F. Donegan, *J. Phys. Chem. C*, 2007, **111**, 14628–14637.

20 S. K. Poznyak, N. P. Osipovich, A. Shavel, D. V. Talapin, M. Gao, A. Eychmüller and N. Gaponik, *J. Phys. Chem. B*, 2005, **109**, 1094–1100.

21 M. P. R. Panicker, M. Knaster and F. A. Kroger, *J. Electrochem. Soc.*, 1978, **125**, 566–572.

22 F. A. Kröger, *J. Electrochem. Soc.*, 1978, **125**, 2028–2034.

23 M. Osial, J. Widera and K. Jackowska, *J. Solid State Electrochem.*, 2013, **17**, 2477–2486.

24 N. P. Osipovich and S. K. Poznyak, *Electrochim. Acta*, 2006, **52**, 996–1002.

25 B. W. Gregory, M. L. Norton and J. L. Stickney, *J. Electroanal. Chem.*, 1990, **293**, 85–101.

26 D. W. Suggs and J. L. Stickney, *J. Phys. Chem.*, 1991, **95**, 10056–10064.

27 E. A. Streltsov, S. K. Poznyak and N. P. Osipovich, *J. Electroanal. Chem.*, 2002, **518**, 103–114.

28 A. S. Bondarenko, G. A. Ragoisha, N. P. Osipovich and E. A. Streltsov, *Electrochem. Commun.*, 2005, **7**, 631–636.

29 G. A. Ragoisha, A. S. Bondarenko, N. P. Osipovich and E. A. Streltsov, *J. Electroanal. Chem.*, 2004, **565**, 227–234.

30 E. A. Streltsov, N. P. Osipovich, L. S. Ivashkevich and A. S. Lyakhov, *Electrochim. Acta*, 1998, **44**, 407–413.

31 J. Aldana, N. Lavelle, Y. Wang and X. Peng, *J. Am. Chem. Soc.*, 2005, **127**, 2496–2504.

32 H. Borchert, D. V. Talapin, N. Gaponik, C. McGinley, S. Adam, A. Lobo, T. Möller and H. Weller, *J. Phys. Chem. B*, 2003, **107**, 9662–9668.

33 G. K. Schweitzer and L. L. Pesterfield, *The Aqueous Chemistry of the Elements*, Oxford University Press, New York, 2010.

This journal is © the Owner Societies 2016

*Phys. Chem. Chem. Phys.*, 2016, **18**, 10355–10361 | 10361